Chemistry of Metals and Alloys

Chem. Met. Alloys 19 (2026) 34-38
ISSN 1998-8079 (print), ISSN 1998-8087 (online)
Ivan Franko National University of Lviv
https://publications.lnu.edu.ua/chemetal

Crystal structure of URu_4Si_2, a new Ru-rich phase in the U–Ru–Si ternary system

Houda EL BEKKACHI[1], Henri NOËL[1], Mathieu PASTUREL[1]*

[1] *University of Rennes, CNRS, Rennes Institute of Chemical Sciences – UMR6226, 35042 Rennes, France*
* *Corresponding author. Tel.:* +33223235861*; e-mail: mathieu.pasturel@univ-rennes.fr*

Received April 30, 2026; accepted June 25, 2026, available online September 9, 2026
https://doi.org/10.30970/cma19.0465

A novel ternary silicide, URu_4Si_2, has been found in the Ru-rich corner of the U–Ru–Si ternary system. It crystallizes in an orthorhombic unit cell, a = 11.1322(4) Å, b = 4.0823(2) Å, c = 9.0612(5) Å, with space group *Pnma* and seven occupied 4*c* atomic positions, corresponding to the YRh_4Ge_2 structure-type, an ordered variant of the $BaHg_6$ type.

Uranium / Ruthenium / Silicide / Crystal structure

1. Introduction

Since the discovery in the mid-1980s of the coexistence of a magnetically ordered state with superconductivity in URu_2Si_2 [1,2], this compound is among the most studied ones in the field of heavy fermion research. Indeed, the real nature of the so-called "hidden" magnetic order and coupling interactions are far from being understood 40 years later [3].

With the aim to find other ternary intermetallic compounds with unconventional physical properties, the U–Ru–Si ternary system is being investigated. In addition to URu_2Si_2, nine other phases are already reported in the literature: URuSi [4], $U_2Ru_3Si_5$ [5], U_2RuSi_3 [6], U_2Ru_3Si [7], $U_6Ru_{16}Si_7$ [8], $U_2Ru_{12}Si_7$ [9], URu_3Si_2 [10,11], $URuSi_{3-x}$ (x = 0.11), and $U_3Ru_{2-x}Si_{7+x}$ ($0 \le x \le 0.39$) [12], two of them ($U_6Ru_{16}Si_7$ and $U_2Ru_{12}Si_7$) located in the Ru-rich corner of the phase diagram. A new ternary phase, URu_4Si_2, has been discovered in this area. Its crystal structure, determined by single-crystal X-ray diffraction, is presented in the following.

Experimental

Polycrystalline samples were prepared by arc-melting stoichiometric amounts of the elemental components (purity above 99.9%) under a protective Ti/Zr-gettered argon atmosphere. Homogenization of the products was performed by long-term annealing (about 1 month) in sealed evacuated silica tubes at 873 K. Small single crystals, suitable for X-ray data collection, were isolated mechanically from the polycrystalline ingots for crystal structure investigations.

Single-crystal X-ray diffraction (XRD) experiments were performed at room temperature on a four-circle Nonius Kappa CCD diffractometer using Mo $K\alpha$ radiation (λ = 0.71073 Å). Reflections collected in a half Ewald sphere were integrated using the Denzo-Scalepack software [13]. The structure was solved by direct methods using the SIR97 software [14] and refined using the SHELXL-97 software [15], after an analytical absorption correction [16].

The quality of the polycrystalline samples was checked by means of X-ray powder diffraction using a Bruker D8 Advance diffractometer working with monochromatized Cu $K\alpha_1$ radiation (λ = 1.5406 Å) and microprobe analysis employing a Jeol JSM 6400 scanning electron microscope equipped with an Oxford 1K EDX spectrometer.

Results and discussion

A ternary phase with composition close to 14U:57Ru:29Si was observed in different as-cast and annealed (down to 873 K) samples synthesized in the Ru-rich corner of the U–Ru–Si phase diagram. Several attempts to obtain phase-pure samples systematically failed, but small single crystals were isolated to perform XRD experiments. Details about data collection and structural refinement are given in Table 1. This compound adopts an orthorhombic structure (*Pnma* space group, no. 62) with lattice parameters a = 11.1322(4) Å, b = 4.0823(2) Å and

Table 1 Crystallographic data and structure refinement for URu_4Si_2.

Empirical formula	URu_4Si_2
Formula weight (g mol^{-1})	698.49
Structure-type	YRh_4Ge_2
Space group	*Pnma*
Unit-cell parameters (Å)	a = 11.1322(4) b = 4.0823(2) c = 9.0612(5)
Unit-cell volume (Å^3)	411.79(3)
Z / calculated density (g cm^{-3})	4 / 11.267
Absorption coefficient, Mo $K\alpha$ (mm^{-1})	53.892
Crystal size (mm×mm×mm)	0.023 ×0.022 × 0.014
Theta range	3.661° to 27.506°
Limiting indices	$-14 \le h \le 14$ $-5 \le k \le 5$ $-11 \le l \le 11$
Collected / unique reflections	903 / 541
R(int)	0.0289
Max. / min. transmission	0.4986 / 0.2703
Data / restraints / parameters	541 / 0 / 43
Goodness of fit on F^2	1.146
R indices [$I>2\sigma(I)$]	$R1$ = 0.0365 $wR2$ = 0.0871
Largest difference peak and hole (e Å^{-3})	+ 3.358 / -3.563

Table 2 Refined atomic parameters and equivalent isotropic displacement parameters (Å^2) for URu_4Si_2 (space group *Pnma*).

Atom	Wyckoff position	x	y	z	Occupancy	U_{eq}
U1	4*c*	0.3288(1)	¼	0.3516(1)	1	0.011(1)
Ru1	4*c*	0.0610(1)	¼	0.3331(2)	1	0.010(1)
Ru2	4*c*	0.2741(1)	¼	0.7069(2)	1	0.010(1)
Ru3	4*c*	0.3386(1)	¼	0.0062(2)	1	0.009(1)
Ru4	4*c*	0.5021(1)	¼	0.6168(2)	1	0.010(1)
Si1	4*c*	0.0603(1)	¼	0.6114(7)	1	0.010(1)
Si2	4*c*	0.1348(5)	¼	0.0905(6)	1	0.009(1)

c = 9.0612(5) Å. There are seven occupied 4*c* Wyckoff positions, one by uranium, four by ruthenium and two by silicon atoms (Table 2), leading to the Pearson symbol *oP*28. The atomic arrangement corresponds to the YRh_4Ge_2 structure-type, described by Voßwinkel *et al*. and adopted by several $RERh_4Ge_2$ [17] and $RERh_4Si_{2-x}Sn_x$ [18] compounds where *RE* is a rare earth, this type being an ordered derivative of the $BaHg_6$-type described by Wendorff and Röhr [19]. URu_4Si_2 appears to be the first reported actinide compound from this family. The ordered crystal structure is thoroughly described by Voßwinkel *et al*., along with its relationship to those of other 1:4:2 stoichiometry phases. A description of the shortest distances within layers parallel to the (*a*,*c*) plane is added here (Fig. 1a). These layers (one at y = ¼ and the next one at y = ¾) contain a strongly bonded sublattice of [Ru5Si3] distorted octagons, sharing edges with two neighboring ones, forming chain-like features propagating along the *a*-axis. These "chains" are separated from one another by [Ru2Si] triangles, [Ru3Si] tetragons and [Ru3Si2] pentagons. Within this skeleton, the Ru-Ru and Ru-Si distances range from 2.347(6) to 2.872(2) Å (Table 3), very close to the sum of the metallic radii of these elements (r_{Ru} = 1.34 Å, and r_{Si} = 1.18 Å [20]). On the contrary, the U atoms occupying the "centers" of the octagons exhibit U-Ru/Si distances ranging from 2.98 to 3.80 Å, above the sum of the metallic radii (r_U = 1.56 Å [20]). Further considering that the U atoms are located between the "centers" of [Ru3Si2] pentagons from the layers situated above and below, with 2×5 additional U-Ru/Si distances ranging from 2.683(2) to 3.229(5) Å, one can define the environment of the U atoms as a large [Ru11Si7] cage (Fig. 1b). From an examination of the database Pearson's Crystal Data [21], one can see that distances between U and ligands ranging from about 2.8 to 3.2 Å are common in ternary compounds associating this actinide, a transition metal (including Ru) and Si or Ge.

Table 3 Selected interatomic distances (Å) in URu_4Si_2.

U1	- 2 Ru2	2.683(2)	Ru2	- 2 Si2	2.511(3)	Ru4	- 1 Si2	2.389(6)
	- 2 Ru4	2.792(2)		- 1 Si1	2.533(5)		- 1 Si1	2.546(6)
	- 1 Ru1	2.986(2)		- 1 Ru4	2.666(2)		- 2 Si2	2.559(3)
	- 2 Si2	3.003(4)		- 2 U1	2.683(2)		- 2 U1	2.792(2)
	- 1 Ru1	3.079(2)		- 1 Ru3	2.806(2)		- 2 Ru1	2.916(2)
	- 1 Ru4	3.082(2)		- 2 Ru1	2.974(2)		- 2 Ru4	2.941(2)
	- 2 Ru3	3.099(2)		- 2 Ru3	3.007(2)		- 2 U1	3.082(2)
	- 1 Ru3	3.131(2)		- 1 U1	3.276(2)			
	- 1 Si2	3.203(6)						
	- 2 Si1	3.229(5)				Si1	- 2 Ru1	2.498(3)
	- 1 Si2	3.447(6)	Ru3	- 1 Si2	2.394(5)		- 2 Ru3	2.518(3)
	- 1 Ru2	3.276(2)		- 2 Si1	2.518(3)		- 1 Ru1	2.522(6)
	- 1 Si1	3.805(6)		- 1 Si1	2.688(5)		- 1 Ru2	2.533(5)
				- 1 Ru2	2.806(2)		- 1 Ru4	2.546(6)
				- 2 Ru1	2.807(2)		- 1 Ru3	2.688(5)
Ru1	- 1 Si2	2.347(6)		- 1 Ru1	2.872(2)		- 2 U1	3.229(5)
	- 2 Si1	2.498(3)		- 2 Ru2	3.007(2)		- 2 Si1	3.169(7)
	- 1 Si1	2.522(6)		- 2 U1	3.099(2)			
	- 2 Ru3	2.807(2)		- 1 U1	3.131(2)			
	- 1 Ru3	2.872(2)				Si2	- 1 Ru1	2.347(6)
	- 2 Ru4	2.916(2)					- 1 Ru4	2.389(6)
	- 2 Ru2	2.974(2)					- 1 Ru3	2.394(5)
	- 1 U1	2.986(2)					- 2 Ru2	2.511(3)
	- 1 U1	3.079(2)					- 2 Ru4	2.559(3)
							- 2 U1	3.003(4)
							- 1 U1	3.447(5)

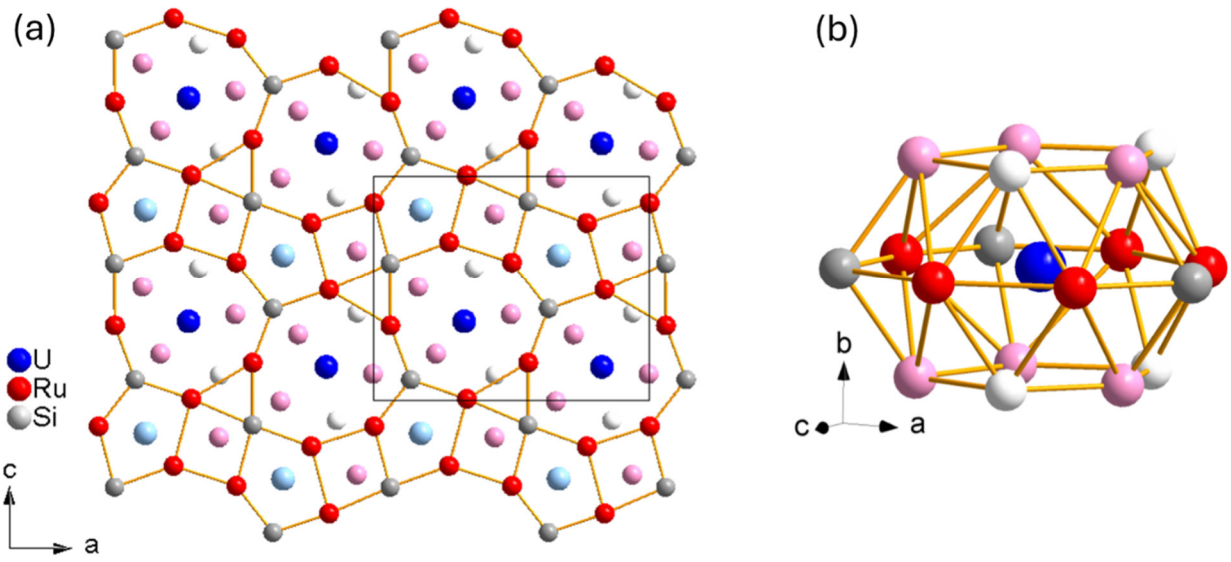


Fig. 1 (a) Crystal structure of URu_4Si_2 viewed along the *b*-axis over several unit cells to highlight the Ru/Si skeleton with short interatomic distances (orange bonds) in layers parallel to the (*a*,*c*) plane and the chain-like features described in the text. (b) [Ru11Si7] environment of the U atoms forming a rather distorted polyhedron with 26 triangular faces and 2 pentagonal ones. In both panels, dark colors indicate atoms at y = ¼ while light colors are used for atoms at y = ¾ and -¼.

Looking at the U-U interatomic distances, the shortest one (4.0823(2) Å) corresponds to the length of the *b*-axis and defines linear rows of U atoms propagating inside [Ru3Si2] pentagonal channels (Fig. 2). Much longer U-U distances of 5.093(1) Å and 5.270(2) Å are found along the above-defined chains and between chains from consecutive layers at z = ¼ and ¾. From these long distances and the high concentration of the non-magnetic d^6 transition metal, no magnetic ordering is expected for this silicide. Accordingly, preliminary measurements of the magnetic susceptibility indicate temperature-independent Pauli paramagnetic behavior, but minor secondary phases still need to be identified to comment on the intrinsic magnetic properties of URu_4Si_2.

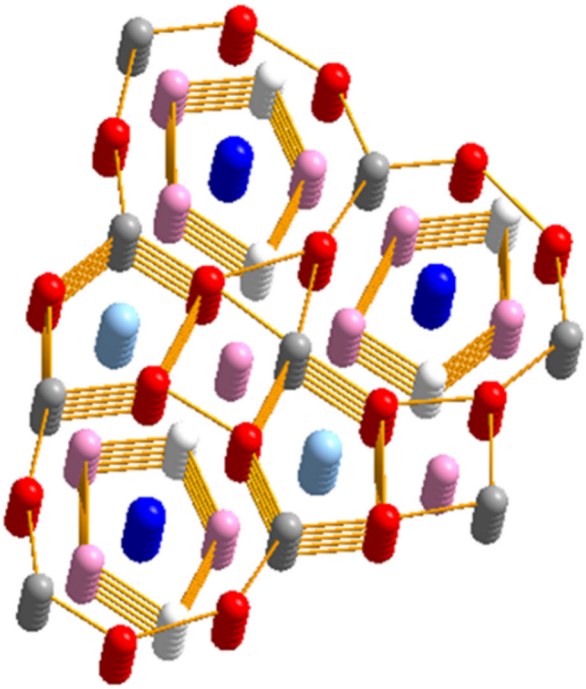


Fig. 2 Crystal structure of URu_4Si_2 showing the chains of U atoms running within pentagonal channels along the *b*-axis. The color code is identical to that used in Fig 1.

Supplementary material

The CIF file can be downloaded from the Crystallography Open Database.

Acknowledgements

Vincent Dorcet is acknowledged for helping us in solving technical problems arising during the building of the CIF file.

References

[1] T.T.M. Palstra, A.A. Menovsky, J. van den Berg, A.J. Dirkmaat, P.H. Kes, G.J. Nieuwenhuys, J.A. Mydosh, *Phys. Rev. Lett*. 55 (1985) 2727-2730. https://doi.org/10.1103/PhysRevLett.55.2727

[2] W. Schlabitz, J. Baumann, B. Pollit, U. Rauchschwalbe, H.M. Mayer, U. Ahlheim, C.D. Bredl, *Z. Phys. B:Condens. Matter* 62 (1986) 171-177. https://doi.org/10.1007/BF01323427

[3] J.A. Mydosh, P.M. Oppeneer, P.S. Riseborough, *J. Phys.:Condens. Matter* 32 (2020) 143002. https://doi.org/10.1088/1361-648X/ab5eba

[4] R. Troć, V.H. Tran, *J. Magn. Magn. Mater*. 73 (1988) 389-397. https://doi.org/10.1016/0304-8853(88)90107-2

[5] E. Hickey, B. Chevalier, P. Gravereau, J. Etourneau, *J. Magn. Magn. Mater*. 90-91 (1990) 501-502. https://doi.org/10.1016/S0304-8853(10)80181-7

[6] R. Pöttgen, P. Gravereau, B. Darriet, B. Chevalier, E. Hickey, J. Etourneau, *J. Mater. Chem.* 4(3) (1994) 463-467. https://doi.org/10.1039/JM9940400463

[7] A. Vernière, P. Lejay, P. Bordet, J. Chenavas, J.P. Brison, P. Haen, J.X. Boucherle, *J. Alloys Compd.* 209 (1994) 251-255. https://doi.org/10.1016/0925-8388(94)91108-8

[8] P. Lejay, A. Vernière, J.X. Boucherle, G. André, *Phys. B* 206-207 (1995) 522-524. https://doi.org/10.1016/0921-4526(94)00509-T

[9] A.V. Zelinskiy, O.I. Bodak, V.M. Davydov, H. Noël, P. Rogl, Yu.D. Seropegin, *Proc. 8th Conf. Crystal Chemistry of Intermetallic Compounds*, Lviv, Ukraine, 2002.

[10] H. Barz, *Mater. Res. Bull.* 15 (1980) 1489-1491. https://doi.org/10.1016/0025-5408(80)90107-5

[11] U. Rauchschwalbe, U. Gottwick, U. Ahlheim, H.M. Mayer, F. Steglich, *J. Less-Common Met.* 111 (1985) 265-275. https://doi.org/10.1016/0022-5088(85)90197-3

[12] M. Pasturel, A.P. Pikul, M. Potel, T. Roisnel, O. Tougait, H. Noël, D. Kaczorowski, *J. Solid State Chem.* 183 (2010) 1884-1890. https://doi.org/10.1016/j.jssc.2010.06.008

[13] Z. Otwinowski, W. Minor, In: C.W. Carter Jr., R.M. Sweet (Eds.), *Methods in Enzymology, Macromolecular Crystallography, part A*, Vol. 276, Academic Press, 1997, pp. 307-326. https://doi.org/10.1016/S0076-6879(97)76066-X

[14] A. Altomare, M.C. Burla, M. Camalli, G.L. Cascarano, C. Giacovazzo, A. Guagliardi, A.G.G. Moliterni, G. Polidori, R. Spagna, *J. Appl. Crystallogr*. 32 (1999) 115-119. https://doi.org/10.1107/S0021889898007717

[15] G.M. Sheldrick, "Programs for Crystal Structure Analysis (Release 97-2)", Institut für Anorganische Chemie der Universität,

Tammanstrasse 4, D-3400 Göttingen, Germany, 1998.
[16] J. de Meulenaar, H. Tompa, *Acta Crystallogr., Sect. A* 19 (1965) 1014-1018. https://doi.org/10.1107/S0365110X65004802
[17] D. Voßwinkel, S.F. Matar, R. Pöttgen, *Monatsh. Chem.* 146 (2015) 1375-1383. https://doi.org/10.1007/s00706-015-1525-5
[18] D. Voßwinkel, C. Benndorf, H. Eckert, S.F. Matar, R. Pöttgen, *Z. Kristallogr.* 231 (2016) 475-486. https://doi.org/10.1515/zkri-2016-1957
[19] M. Wendorff, C. Röhr, *J. Alloys Compd.* 546 (2013) 320-328. http://dx.doi.org/10.1016/j.jallcom.2012.07.101
[20] E. Teatum, K. Gschneidner, J. Waber, *Compilation of calculated data useful in predicting metallurgical behavior of the elements in binary alloy systems*, Los Alamos Scientific Laboratory, LA-2345, USA, 1960.
[21] P. Villars, K. Cenzual (Eds.), *Pearson's Crystal Data – Crystal Structure Database for Inorganic Compounds*, Release 2019/20, ASM International, Materials Park, Ohio, USA.

Authors and ORCID IDs:
Houda EL BEKKACHI: –
Henri NOËL: 0009-0001-1858-9584
Mathieu PASTUREL: 0000-0002-2172-9533

The paper is distributed under the terms of the Creative Commons Attribution Non-Commercial 4.0 (CC BY-NC) international license.